THE JOURNAL OF PHYSICAL CHEMISTRY A

pubs.acs.org/JPCA Article

The Connectivity Matrix: A Toolbox for Monitoring Bonded Atoms and Bonds

Published as part of The Journal of Physical Chemistry virtual special issue "Paul Geerlings Festschrift".

Piotr Ordon, Ludwik Komorowski,* Mateusz Jędrzejewski, and Jarosław Zaklika

Cite This: *J. Phys. Chem. A* 2020, 124, 1076–1086 Read Online

ACCESS | Metrics & More | Article Recommendations

ABSTRACT: The concept of a connectivity matrix, essential for the reaction fragility (RF) spectra technique for monitoring electron density evolution in a chemical reaction, has been supported with a novel formulation for the diagonal matrix elements; their direct link to the electron density function $\rho(\mathbf{r})$ has been demonstrated. By combining the concept with the atomization energy of a system, the separation of the potential energy into atomic and/or bond contributions has been achieved. The energy derivative diagrams for atoms and bonds that are variable along a reaction path provide new insight into the reaction mechanism. Diagonalization of the connectivity matrix resulted in the eigenvectors that provide information on a role of individual atoms in the development of structural changes along a reaction path.

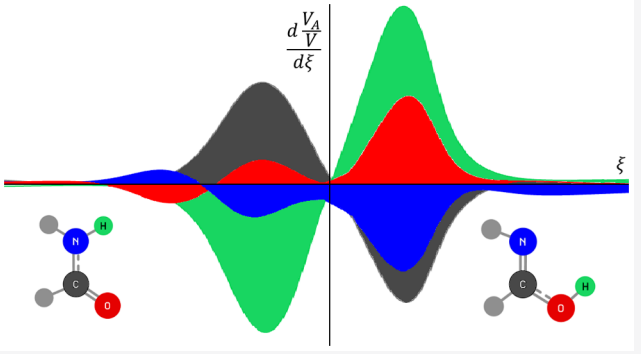

1. INTRODUCTION

Politzer and Murray focused their recent paper on the distinction between the concept of a bond, the central issue for chemical knowledge, and the much broader physical idea of bonding interaction.[1] In a very concise yet very enlightening manner the authors outline relevant key points in the development of the growth of quantum theory, from the fundamental mathematical idea of the wave function to the reality of the electron density function: from Schrödinger through Feynman, Hohenberg and Kohn to Bader[2−7] They noticed numerous critical views concerning the very idea of an atom-in-molecule[8−10] and their connections, that for more than a century have been known in chemistry as "bonds".[11−14]

This very general review provides an opportunity to recall an even broader topic, essential from the chemical point of view: the bond reorganization in a reaction. There has been growing interest in monitoring the change of the electronic structure in an array of atoms undergoing a change between two equilibrium states, RS (reagent state) and PS (product state), respectively. Wide access to computational methods has been opened by the intrinsic reaction coordinate (IRC) formalism,[15−17] that allows for observation not only the energy but also the structure of the system undergoing a change. While discussion to what extent the IRC formalism can reproduce reality remains open,[18,19] the method has attracted attention at various levels of the approach based on the potential energy surface (PES).[20] The simple one has been focused on analysis of the energy derivatives over reaction progress (ξ) as defined by the IRC formalism[21−24] (reaction force, $F_\xi = -dE/d\xi$; reaction electronic flux, $J = -dE^2/dNd\xi$). The more sophisticated attempt produced a complete analysis of normal vibrational modes at the reaction steps and focused on factors stimulating their evolution upon a reaction.[25−27] To gain attention from the chemical community, both types of research had to cope with the challenge of identifying atoms/bonds in their results. For the energy derivatives, the QTAIM approach has been arbitrarily advocated as a working concept in identifying the atomic contributions;[28,29] otherwise, interacting quantum atoms (IQA) have been proposed.[30] An early study on atomic contributions to the reaction force has demonstrated a relation thereof to atomic charges provided by standard population analyses.[31]

The separation of individual bonds within the normal-mode analysis has been elaborated by the unified reaction valley approach (URVA) by Kraka and collaborators.[32] They demonstrated how the evolution of scalar curvature of the reaction path allows for identification of the individual bond formation/cleavage as a reaction proceeds.[33] This was built on the concept of adiabatic internal vibrational modes (AIMO),[34]

Received: October 29, 2019
Revised: December 10, 2019
Published: January 21, 2020

https://dx.doi.org/10.1021/acs.jpca.9b10145
J. Phys. Chem. A 2020, 124, 1076–1086

the stretching modes for selected bonds complying with the symmetry of the molecule and extracted from the entire structure of normal modes. Decomposition of normal modes into adiabatic curvature coefficients tentatively assigned to bonds allowed for observation of the chemical changes in the reaction complex with the reaction progress; bond forming and breaking was also observed by the electron density analysis within the QTAIM framework.[20]

The present authors have proposed another original solution for identification of atoms/bonds in a molecular system; it has been based on the Hellmann−Feynman definition of force acting on each nucleus $\mathbf{F}_A^{\mathrm{H-F}}$ (H−F force). While the identity of a bonded atom is vague, the location of its nucleus and the force acting on it have firm physical reality, as Feynman had demonstrated:[3,35−38]

$$\mathbf{F}_A^{\mathrm{H-F}} = -\nabla_A E = \int \rho(\mathbf{r})\, \boldsymbol{\varepsilon}_A(\mathbf{r})\, \mathrm{d}\mathbf{r} + \mathbf{F}_A^{n-n} \tag{1}$$

$\mathbf{F}_A^{\mathrm{n-n}}$ is the nuclear repulsion force on the nucleus "A" and $\nabla_A E$ stands for the energy gradient vector. Most important is the role of the electron density function for the whole system $\rho(\mathbf{r})$, in the attracting force on the nucleus (the integral in eq 1); it contains the vector of electric field generated by the nucleus in question only $\boldsymbol{\varepsilon}_A(\mathbf{r})$. By the Hohenberg−Kohn theorem, $\rho(\mathbf{r})$ is uniquely characteristic for the actual configuration of the nuclei. $\mathbf{F}_A^{\mathrm{H-F}}$ force vector is identically zero on each atom in the equilibrium configuration of the nuclei; in the stationary states of the electron density at arbitrary position of nuclei (e.g., points on IRC), the forces on the nuclei $\mathbf{F}_A^{\mathrm{H-F}}$ are not zero.

The vector formulation of force in eq 1 exposed by the present authors[39] is crucial for application of eq 1 to the systems undergoing changes on a reaction path. When the divergence of the H−F force vector (a number) is calculated, the contribution from the internuclear forces ($\mathbf{F}_A^{\mathrm{n-n}}$ in eq 1) vanishes, since $\nabla_B \cdot \mathbf{F}_A^{\mathrm{n-n}} = 0$ by the Laplace theorem. The result is

$$\nabla_B \cdot \mathbf{F}_A^{\mathrm{H-F}} = \nabla_B \cdot \int \rho(\mathbf{r})\, \boldsymbol{\varepsilon}_A(\mathbf{r})\, \mathrm{d}\mathbf{r} \tag{2}$$

The electric field of the nucleus $\boldsymbol{\varepsilon}_A(\mathbf{r})$ (eq 2) does not vary upon a change of the position of this nucleus $\nabla_A \cdot \boldsymbol{\varepsilon}_A(\mathbf{r}) = 0$; the field $\boldsymbol{\varepsilon}_A(\mathbf{r})$ provides a constant frame for the electron density function variable upon the change. Hence, the divergence of force calculated for each atom of a reacting system ($\nabla_A \cdot \mathbf{F}_A^{\mathrm{H-F}}$ in eq 2) carries information (hidden in the electron density function $\rho(\mathbf{r})$), on the identity of each bonded atom that is modified when the reaction proceeds. Equation 2 also provides a clear-cut condition for the "limit of bonding", by considering the divergence $\nabla_{B\neq A} \cdot \mathbf{F}_A^{\mathrm{H-F}}$. Two atoms must be considered nonbonded when a virtual displacement of one atom would not alter the integral calculated for the second atom (eq 2). By definition $\nabla_{B\neq A} \cdot \boldsymbol{\varepsilon}_A(\mathbf{r}) = 0$; hence, the result $\nabla_{B\neq A} \cdot \mathbf{F}_A^{\mathrm{H-F}} = 0$ means that disturbance of the position of atom B does not affect the density function in the integral (eq 2).

This disarming argument provided a hint to exploration of the divergences of the H−F forces over the atomic positions in tracing changes in atoms and bonds along a reaction path. The computational method has been proposed for monitoring the divergences (eq 2) along a reaction path by the diagrams presenting the derivatives for atoms and bonds respectively: $a_\xi^A = \mathrm{d}(\nabla_A \cdot \mathbf{F}_A^{\mathrm{H-F}})/\mathrm{d}\xi$ and $a_\xi^{AB} = -\mathrm{d}(\nabla_B \cdot \mathbf{F}_A^{\mathrm{H-F}})/\mathrm{d}\xi$. Persuasive pictures for bond formating/breaking along IRC have already been demonstrated for several reactions as the reaction fragility (RF) spectra for atoms and bonds.[39,40,43,44]

The aim of this work is to review briefly the properties of the divergences (eq 2) collected in the connectivity matrix for a system, in order to demonstrate their new explicit relation to the electron density function (section 2). Application of the concept to tentative separation of the potential energy of a system into atomic contributions and their observation in a system undergoing a reaction has been presented in sections 3 and 4.

2. THE CONNECTIVITY MATRIX

Calculation of the divergences of $\mathbf{F}_A^{\mathrm{H-F}}$ forces (eq 2) for any system of atoms is straightforward: they are produced directly as sums of appropriate elements of the Cartesian Hessian; the results must be invariant, being the scalar products.

$$\begin{aligned}\nabla_B \cdot \mathbf{F}_A^{\mathrm{H-F}} &= \frac{\partial F_{A,x}}{\partial R_{B,x}} + \frac{\partial F_{A,y}}{\partial R_{B,y}} + \frac{\partial F_{A,z}}{\partial R_{B,z}} \\ &= k_{xx}^{BA} + k_{yy}^{BA} + k_{zz}^{BA} \\ &\equiv C_{BA}\end{aligned} \tag{3}$$

This calculation procedure (eq 3) has justified the name *cumulative force constants* introduced for the divergences ($B \neq A$).[39] They form an $n \times n$ matrix for a system of n atoms: $\underline{\underline{\mathbf{C}}}$, the connectivity matrix. If there is no connection between atoms, the corresponding matrix elements vanish: $C_{AB} = C_{BA} = 0$. An important property of the matrix has been proven:[39]

$$C_{AA} = -\sum_{B\neq A} C_{BA} \tag{4}$$

This is a consequence of the vanishing total force in a system of interacting atoms. It makes the determinant of the matrix equal zero; hence, the $\underline{\underline{\mathbf{C}}}$ matrix is singular.

Equation 4 indicates that the connectivity matrix not only provides a comprehensive, quantitative description for bonds (eq 3, cumulative force constants) but also provides an analogous parameter for the bonded atoms themselves (C_{AA}). The trace of the connectivity matrix is identical to the trace of the original Cartesian Hessian and also to the Wilson matrix resulting from the normal mode transformation. However, unlike the other two matrices, the diagonal elements of the $\underline{\underline{\mathbf{C}}}$ matrix exposes directly the degree of being bonded for individual atoms (C_{AA}) in a similar manner as the cumulative force constants do for contacts between atoms ($C_{B\neq A}$), eq 4. The linear relation of $C_{B\neq A}$ to the Wiberg bond indices and C_{AA} to atomic valences as defined by Mayer,[41] has been documented.[43,44] Without defining atoms, the connectivity matrix provides a well understood physical measure of their bonding power (force constant analogue), thus resolving the ambiguity: bonds appear to be a particular form of bonding; a bond is characterized by a strong enough interaction measured by $C_{B\neq A}$.

Explicit relations between the divergences of H−F force (eqs 2 and 3) and the electron density function have been demonstrated:[39]

$$C_{AA} = 4\pi Z_A \rho(\mathbf{R}_A) + \int \boldsymbol{\varepsilon}_A(\mathbf{r}) \cdot [\nabla_A \rho(\mathbf{r})]_N\, \mathrm{d}\mathbf{r} \tag{5}$$

$$C_{B\neq A} = \int \boldsymbol{\varepsilon}_A(\mathbf{r}) \cdot [\nabla_{B\neq A} \rho(\mathbf{r})]_N\, \mathrm{d}\mathbf{r} \tag{6}$$

The role of density at the nucleus in eq 5 has been unclear, since $\rho(\mathbf{R}_A) \neq 0$, it may be eliminated, by exploring the general result elaborated by Liu et al.[45]

https://dx.doi.org/10.1021/acs.jpca.9b10145
J. Phys. Chem. A 2020, 124, 1076−1086

$$\rho(\mathbf{R}_A) = -\frac{1}{4\pi}\int \frac{(\mathbf{r}-\mathbf{R}_A)\cdot\nabla\rho(\mathbf{r})}{|\mathbf{r}-\mathbf{R}_A|^3}\,\mathrm{d}\mathbf{r} \tag{7}$$

By using this result, eq 5 is transformed to a novel form containing the electron density function $\rho(\mathbf{r})$ as the only variable parameter on the reaction path for the diagonal elements of the connectivity matrix (eq 8); an elegant pendant to the expression for the nondiagonal elements of the connectivity matrix (eq 6).

$$C_{AA} = \int \boldsymbol{\varepsilon}_A(\mathbf{r})\cdot[\nabla\rho(\mathbf{r}) + \nabla_A\rho(\mathbf{r})]_N\,\mathrm{d}\mathbf{r} \tag{8}$$

Since for a single atom $\nabla\rho(\mathbf{r}) = -\nabla_A\rho(\mathbf{r})$, eq 8 properly explains why $C_{AA} = 0$ for a noninteracting atom. When other sources of electric field are present, for example, other nuclei nearby, $C_{AA} > 0$ as has been demonstrated by the connectivity matrices.[39] However, the integral in eq 8 calculated for an atom can be finite if, and only if

$$\lim_{\mathbf{r}\to 0}[\nabla\rho(\mathbf{r}) + \nabla_A\rho(\mathbf{r})] = 0 \tag{9}$$

since $\boldsymbol{\varepsilon}_A(\mathbf{r}) \to \infty$ for $\mathbf{r} \to 0$. The cusp condition[46,47] requires $\nabla\rho(0)$ to be finite, hence an additional general condition emerges for the electron density at a nucleus:

$$\lim_{\mathbf{r}\to 0}\nabla\rho(\mathbf{r}) = -\lim_{\mathbf{r}\to 0}\nabla_A\rho(\mathbf{r}) \tag{10}$$

Exact results for the connectivity matrix elements (eq 8 and eq 6) provide valuable and much needed justification for the practically observed variations of the elements of the connectivity matrix (both C_{AA} and $C_{B\neq A}$), on the reaction progress (IRC), when a system undergoes a reaction: the reaction fragility (RF) profiles. Without a need for identification of individual atoms, the C_{AA} elements in the matrix report the density modifications around each atom as the reaction proceeds, since the electric field around an atom does not change upon the reorganization of the nuclei,[39]

$$\mathrm{d}\boldsymbol{\varepsilon}_A(\mathbf{r})/\mathrm{d}\xi = 0 \tag{11}$$

3. THE NEW METHOD: EXTRACTING ATOMIC AND BOND CONTRIBUTIONS TO THE ENERGY OF A MOLECULE

The connectivity matrix ($\underline{\underline{\mathbf{C}}}$) for a collection of noninteracting atoms is trivially zero. For a diatomic molecule it is a 2 × 2 matrix, with only one nontrivial value k:

$$C_{AA} = C_{BB} = k = \frac{1}{2}\mathrm{Tr}\underline{\underline{\mathbf{C}}} \quad \text{and} \quad C_{AB} = C_{BB} = -k \tag{12}$$

As Politzer and Murray have reminded, the energy (E) of a system in a stationary state of electron density is exactly measured by its potential energy $E = {}^1/_2V$ (by the virial theorem); hence, the derivatives of E and V over the reaction progress are equivalent. The model potential energy curve $V(x)$ for a diatomic molecule A−B has been provided by the Morse' function, properly accounting for the dissociation process ($x = |\Delta\mathbf{R}_{AB}|$):

$$V(x) = D_e[1 - \exp(-ax)]^2 \tag{13}$$

In molecules this function has been commonly used to describe individual bonds by providing two parameters for a chosen bond: dissociation energy D_e and the Morse coefficient $a > 0$. They describe sufficiently well the potential energy derivative $V'' = \mathrm{d}^2V/\mathrm{d}x^2$ near the energy minimum. The force constant is directly related to the parameters in eq 13:

$$V'' = k = 2D_e a^2 \tag{14}$$

The third derivative, $V''' = -3ka < 0$ provides a practical measure of the anharmonicity of a bond. An alternative measure of anharmonicity, the spectroscopic anharmonicity constant (x_e) is also directly related to the Morse coefficient (a): $x_e = a^2h/2\pi\mu\omega$.[48] The simplicity of the model justified its wide application, even though the concept of breaking one bond only is hardly realistic.

The connectivity matrix allows for extending the Morse concept to a molecule as a whole, considering its global expansion; the process of complete dissociation to atoms is somewhat more realistic than single-bond breaking. Specification of a detailed shape of the potential energy function $V(\Delta\mathbf{R}_1,\Delta\mathbf{R}_2,...)$ is not required for application of the model; the scalar argument $x > 0$ may conveniently be defined for a whole system, such as, $x = \sqrt{\sum_{\mathrm{bonds}}(\Delta\mathbf{R}_{AB})^2}$. This is equivalent to tracing a specific path for the expansion process, leading to its final result—the disintegration of a molecule to atoms. The well-defined atomization energy (D_{at}) may be used for the global dissociation energy and the $\frac{1}{2}\mathrm{Tr}\underline{\underline{\mathbf{C}}}$ value may replace the force constant (k) in eq 14. This is sufficient to calculate the global Morse parameter for the entire system a_M (eq 15). Since the elements of the connectivity matrix are typically calculated from the energy (E), rather than from the potential energy (V), factor 2 must be included in the final result:

$$(a_M)^2 = \frac{1}{8D_{\mathrm{at}}}\sum_A^{\mathrm{atoms}} C_{AA} \tag{15}$$

This unique parameter is sufficient for identification of atomic contributions to the atomization energy ($D_{at,A}$).

$$D_{\mathrm{at}} \equiv \sum_A^{\mathrm{atoms}} D_{\mathrm{at},A} \quad \text{where } D_{\mathrm{at},A} = \frac{C_{AA}}{8(a_M)^2} \tag{16}$$

Since the atomization energy is independently calculated, the dimensionless terms $C_{AA}/\sum_A C_{AA}$ provide information on the atomic share in the overall atomization energy of a system, variable along a reaction path, thus also to a role of an atom in the reaction. By the Morse' eq (eq 13), this is equivalent to separation of the potential energy to atoms $V = \Sigma V_A$.

$$\frac{V_A}{V} = \frac{D_{\mathrm{at},A}}{D_{\mathrm{at}}} = \frac{C_{AA}}{\sum_A C_{AA}} \tag{17}$$

An analogous procedure can be extended to bonds, by combining eq 4 and eq 17. Since the connectivity matrix is symmetric, the contributions from bonds to $\mathrm{Tr}\underline{\underline{\mathbf{C}}}$ are doubled.

$$\frac{V_{AB}}{V} = -\frac{2C_{AB}}{\sum_A C_{AA}} \tag{18}$$

Equations 17 and 18 expose an additional feature of the connectivity matrix calculated along a reaction path: it may allow for observation of the relative energy of individual atoms or bonds by tracing variations of the individual shares of atoms (bonds) in the overall energy of the system, given by the derivatives $d(C_{AA}/\mathrm{Tr}\underline{\underline{\mathbf{C}}})/d\xi\mathrm{vs}\xi$ and $d(-2C_{AB}/\mathrm{Tr}\underline{\underline{\mathbf{C}}})/d\xi\mathrm{vs}\xi$. The relation between such diagrams of energy derivatives and the fragility spectra established in earlier works

https://dx.doi.org/10.1021/acs.jpca.9b10145
J. Phys. Chem. A 2020, 124, 1076−1086

Table 1. Calculated Transition State Energies (ΔE_{TS}) and Reaction Energies (ΔE). Atomization Energies (D_{at}) for the Reactant State (RS) and Product State (PS) of the Reaction Have Also Been Included

						D_{at} [au]	
molecule	reaction	no.	ΔE_{TS} [kcal/mol]	ΔE [kcal/mol]	ref	RS	PS
H_2NCHO	(ROT)	**R1**	18.75	0	50, 51	1.0746	1.0746
H_2NCHO	(PT)	**R2**	45.93	12.24	50, 51	1.0746	1.0551
$(H_2NCHO)\cdot(H_2O)$	(DPT)	**R3**	22.14	10.63	50, 51	1.5590	1.5420

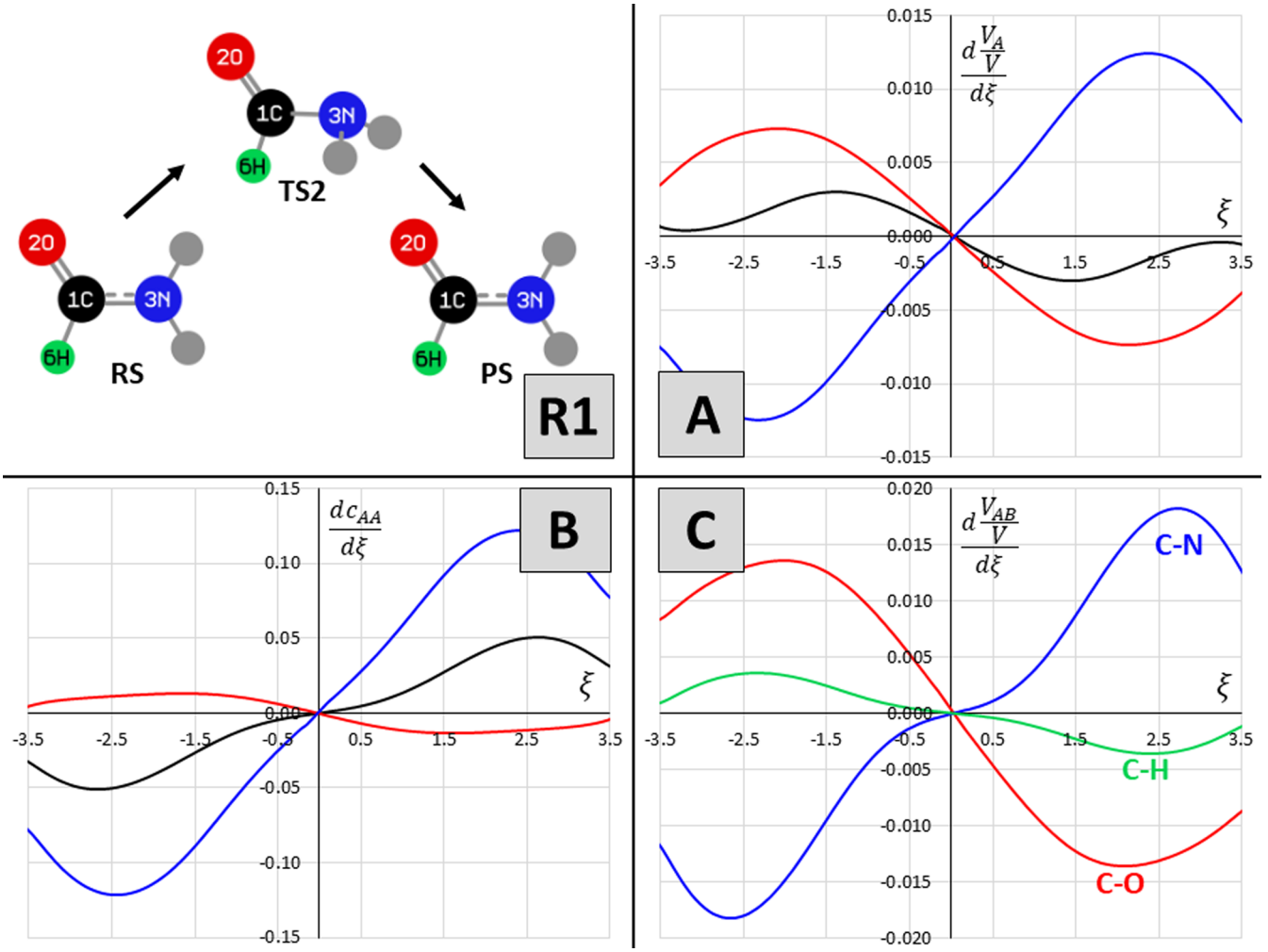

Figure 1. Energy derivative diagrams (in au) for atoms (eq 17, A) and bonds (eq 18, C) in the formamide rotation (**R1**) as compared the RF atomic spectra (B) for this reaction (the color codes of atoms in R1 have been repeated for lines in diagrams A and B).

($a^A_\xi = dC_{AA}/d\xi$ vs ξ) is not trivial, as the trace of the matrix (Tr$\underline{\underline{\mathbf{C}}}$) is itself considerably variable in the reaction.[40]

4. RESULTS AND DISCUSSION

The formamide molecule has been chosen for a working example for three types of reactions: an internal rotation (ROT) around the C−N bond (**R1**), an internal proton transfer (PT) between NH_2 and CO groups (**R2**), and the double proton transfer (DPT) mediated by a water molecule (**R3**). The set of three types of well understood processes involving the same molecule (NH_2CHO) allows for testing the results of the proposed method of energy separation between atoms; the fragility spectra for these three processes have been reported separately.[42,43] Evolution of eigenvalues and the corresponding eigenvectors of the connectivity matrix at three key stages of the reaction (RS → TS → PS) has been presented for the internal proton transfer reaction in formamide (**R2**).

The connectivity matrix has been obtained from the IRC energy profile reproduced by the standard procedure (QST2) at the MP2 level using the 6-311++G(*3df,3pd*) basis set and the Gaussian 09 code.[49,17] The Cartesian Hessian elements have been calculated for single points using the geometry of the structures resulting on the IRC. The TS2 transition state has been considered for **R1**.[43] Proton transfer in the formamide molecule (**R2**) has been considered in the planar configuration, as established in the literature. For the formamide/water complex (**R3**), the planar configuration has been adopted.[50,51] The results for the transition state energies (ΔE_{TS}) and the reaction energies (ΔE) in Table 1 demonstrate the much different nature of these reactions.

https://dx.doi.org/10.1021/acs.jpca.9b10145
J. Phys. Chem. A 2020, 124, 1076−1086

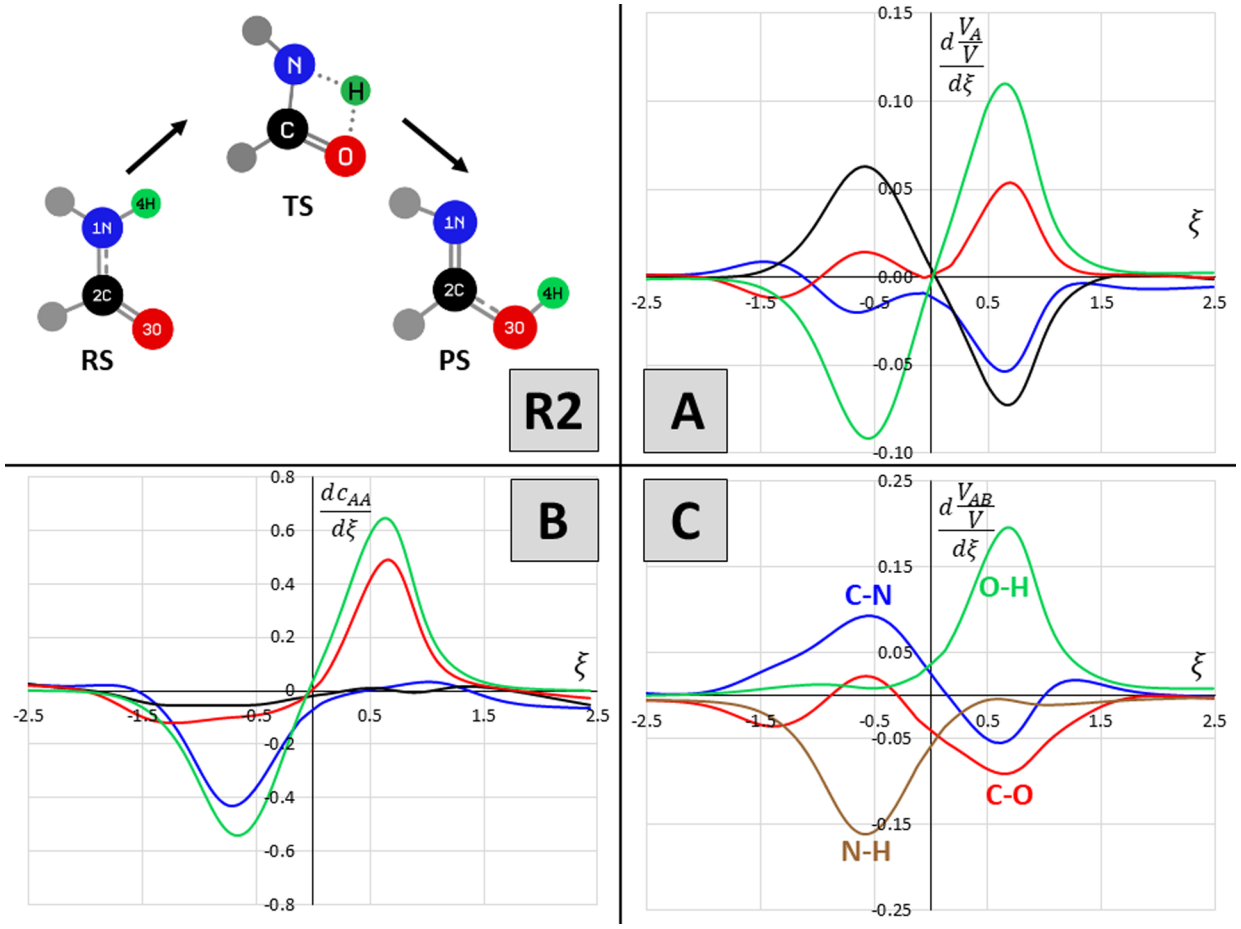

Figure 2. Energy derivative diagrams (in au) for atoms (eq 17, A) and bonds (eq 18, C) in the internal proton transfer in formamide molecule (**R2**), as compared to the RF atomic spectra (B) for this reaction (the color codes of atoms in **R2** have been repeated for the lines in diagrams A and B).

Results reported in Table 1 have been supplemented by calculation of the atomization energies (D_{at}) for the equilibrium states (RS and PS) in the reactions under study. Atomization energies have recently been recalled as an important source for chemical information.[52] The atomic energies were calculated at the same level of the theory as molecular energies; results were in excellent agreement with the average of the corrected data reported by Csonka et al. obtained with several advanced methods with the same basis set as is used in this work.[53] Deviations of our results from the average results by the above authors were less than standard deviations in their data.

Diagrams of Relative Energy Derivatives for Atoms and Bonds. Proportionality between atomization energy and the trace of the connectivity matrix analogous to the one for the original Morse' equation (eq 14) is a precondition for application of the Morse' model to atomization energy. This has been tested by examination of the linear relation between atomization energy D_{at} and $\frac{1}{2}\mathrm{Tr}\underline{\underline{\mathbf{C}}}$ replacing the dissociation energy (D_e) and the force constant (k), respectively (eq 14). The collection of 25 molecules representing the reagent and product states of the reactions previously explored for investigation of the fragility spectra has been used for testing the correlation.[43,44] The formamide and the formic acid molecules skeletons (N−C−X and X−C−Y where X,Y = O,S, respectively) are common building motives in this collection. Structural proximity of the chosen systems is intentional: the Morse' anharmonicity coefficient a (eq 14) is formally characteristic for a bond; hence, its analogue for a molecule a_M may vary between molecules. The chosen molecules are formamide and its substituted analogues[43] (5), formamide water complex (2), formamide and thioformamide complexes (6), thioformic acid[44] (2), and mixed dimers of formic and thioformic acids[44] (10). Atomization energies in this collection covered the range [0.770−2.20 au], while the $Tr\underline{\underline{\mathbf{C}}}$ values were [3.74−11.9 au]. Assuming the relation in the form $\frac{1}{2}Tr\underline{\underline{\mathbf{C}}} = \alpha D_{at}$ according to the requirement of eq 14, the result for the slope was: α = 2.34 (±0.07) $(a_o)^{-2}$ at R^2 = 0.980 (a_o stands for the Bohr unit of distance). This correlation parameter implies an average value for the Morse coefficient in the collection of bonds (eq 15): a_M = 2.04 Å^{-1}. This result for an effective anharmonicity parameter characterizing the entire system on its way to complete dissociation into atoms appears to be quite realistic as compared to results in diatomic molecules.[54]

The relative shares in the global potential energy attributed to atoms in a reacting system (V_A/V) and bonds (V_{AB}/V) have been calculated according to eq 17 and eq 18, respectively. The energy derivatives diagrams $d(V_A/V)/d\xi$ and $d(V_{AB}/V)/d\xi$ along the reaction path have been shown together with the corresponding reaction fragility (RF) atomic spectra, $a_\xi^A = dC_{AA}/d\xi$. Results have been shown in Figures 1, 2, and 3. The derivatives represent the pace of changes in V_A/V rather than the values themselves.

Atomic RF spectra for the internal rotation (Figure 1B) demonstrate the electron density shift from C atom toward O

https://dx.doi.org/10.1021/acs.jpca.9b10145
J. Phys. Chem. A 2020, 124, 1076−1086

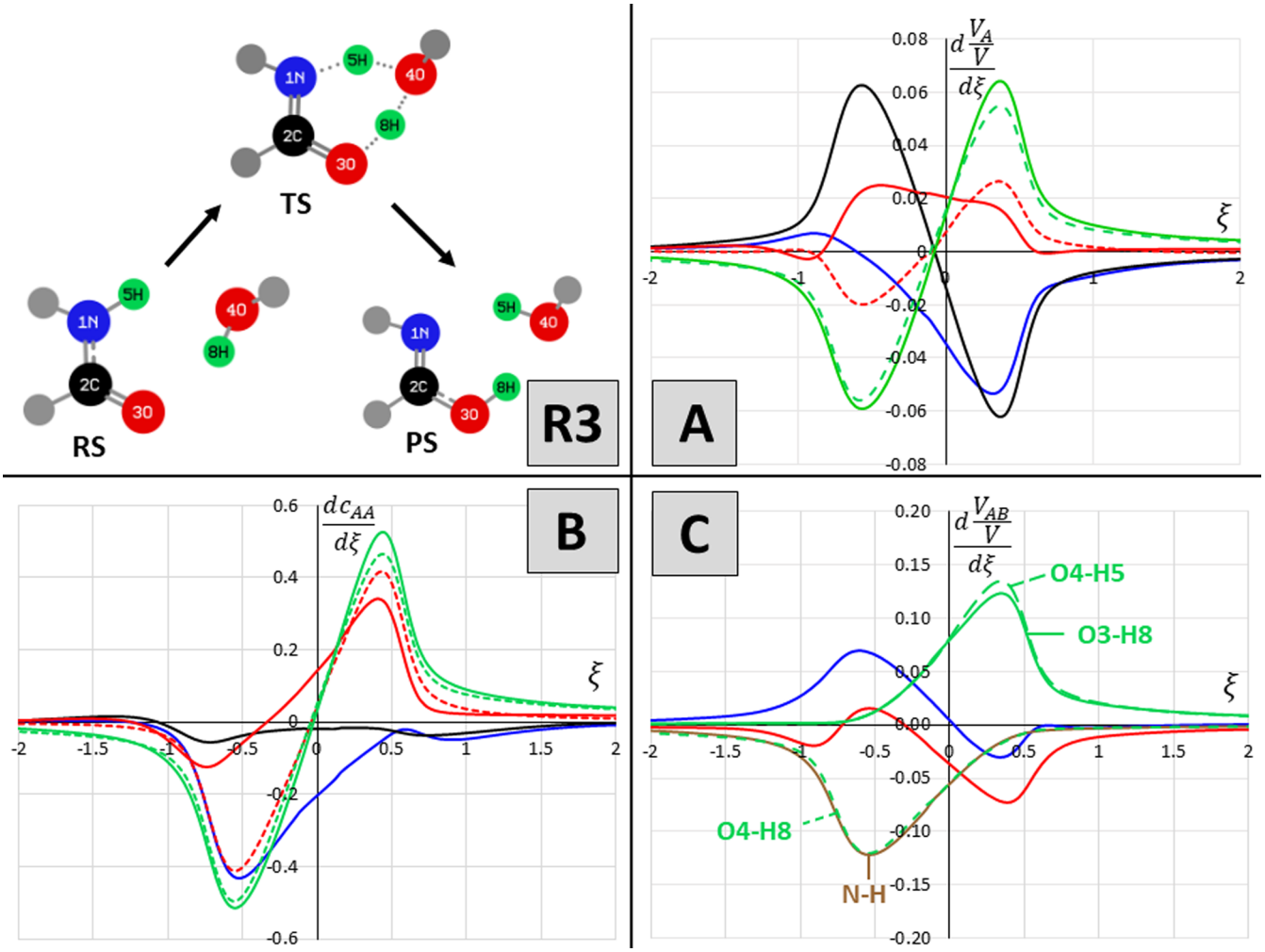

Figure 3. Energy derivative diagrams (in au) for atoms (eq 17A) and bonds (eq 18C) in the double proton transfer in formamide/water complex (**R3**), as compared to the RF atomic spectra (B) for this reaction. (The color codes of atoms in R3 have been repeated for the lines in diagrams A and B; the solid red and green lines in A and B are for 3O and 5H atoms, while the dashed lines are for 4O and 8H atoms, respectively.).

and N atoms in O−C−N skeleton upon rotation around the C−N bond to the TS (90°). This is associated with the increase of the energy of O atom (Figure 1A) as the C−O bond becomes stronger (Figure 1C), while the energy of the N atom and C−N bond decreases (Figure 1A,C). The net increase of the energy of C atom (Figure 1A) is notable, as it appears to be a consequence of the increase in O−C and H−C bonds energy (Figure 1C), despite the energy decrease in the C−N bond that affects energy of the N atom, exclusively.

For the internal proton transfer reaction (**R2**) the energy derivative diagrams disclose more details than the RF spectra (Figure 1B). At the initial stage of this reaction, with the H4 hydrogen atom drifting away from the N atom, all atoms in the system experience a loss of the electron density, as shown in their RF spectra (Figure 2B). When the H4−N bond is being broken (Figure 2C), the C−N bond energy increases, while the C−O bond energy is initially lowered. This trend is inversed as early as at ca. $\xi \cong -1.5$, apparently under the influence of the H4 atom aiming toward oxygen. The energy derivative spectra of the C, O, and N atoms provide an interesting picture of the evolution of bonding of these atoms (Figure 2A). The energy derivative for the carbon atom tends to a maximum at ca. $\xi \cong -0.5$, and the effect is strong enough to warrant the steady C−N bond energy derivative increase, but not for the C−O energy. A competition between bonding of N and O to carbon is evidenced by their atomic energy derivatives: two consecutive maxima and minima in the N atom are accompanied by corresponding minima and maxima in the O atom at ca. $\xi \cong -1.4$, -0.5, 0, and -0.5, respectively. The extremes in the nitrogen atom energy derivatives occur typically by 0.1 unit ξ earlier than for the oxygen atom; this interesting dynamics must be a consequence of H4 atom displacement on its way from N to O atoms.

At $\xi \cong -0.5$ the energy derivatives of C−O and C−N bonds reach their maxima, with an associated minimum for the H4−N bond, meaning the turning point for abstraction of H4 hydrogen on its way (Figure 2C). This is perfectly well confirmed by the minimum on the H4 atom energy derivative at the same point ($\xi \cong -0.5$, Figure 2A). The maxima on the C and O curves in the same point complete the evidence. The final stage of the process that begins at ca. $\xi \cong -0.5$ is clearly envisaged by the atomic energy derivative diagrams (Figure 1A): Oxygen and H4 atoms strengthen their energy, while C and N atoms lose it, proportionally.

A valuable observation for bond-energy derivatives is found in Figure 2C. Unlike the atomic energy derivatives (Figure 2A), the bond energy derivative diagrams do not tend to zero at $\xi = 0$ energy. These nonzero derivatives of relative bond energies disclose an important feature of this process: its structural

https://dx.doi.org/10.1021/acs.jpca.9b10145
J. Phys. Chem. A 2020, 124, 1076−1086

turning points do not coincide with the global energy-based TS point for the entire process.

The general picture of the double proton transfer reaction (**R3**) provided by the energy derivatives for atoms and bonds in this reaction fully corroborates the observations for the simple proton transfer (**R2**). Fragility spectra for all atoms illustrate the density loss when approaching the transition state (Figure 3B); the turning point of the process is again at ca. $\xi \cong -(0.5-0.6)$, and $\xi \cong 0.4$ for the final stage of the process. The profiles for the N−C−O atoms are not symmetric: nitrogen (N1) loses its density to a much greater degree that oxygen (O3), and carbon (C2) shows only a minute decrease in the density.

The energy derivatives of atoms (Figure 3A) indicate that, despite the loss in density, the N1 atom energy is not affected in the (RS, TS) region; it is compensated by the increase in N−C and C−O bond-energy derivatives (Figure 3C); this is confirmed by the energy derivative of the carbon atom (Figure 3A). Increasing the bond energy derivative with the parallel density loss hints to the ionicity of the bond, and this indeed is the case: the negative charge on the nitrogen atom (Hirshfeld) increases by 50% between RS and TS.

The new element here is an opportunity to see two oxygen atoms in various environments participating in the process. As might be expected, their response to the hydrogen atom transfers is concerted. By the RF spectra (Figure 3B), the density around the O3 atom in the O−C−N backbone is considerable less affected by the process than at the O4 oxygen atom in the associated water molecule although the gradual changes in the fragility are parallel for these atoms; the oxygen atom in the O−C−N backbone apparently enjoys the screening effect by the neighboring C atom, the energy derivative of which increases substantially.

The notable differences between O3 and O4 atoms have been exposed by their atomic energy derivatives (Figure 3A). The oxygen atom in the water molecule (O4) loses energy in the initial stage of the reaction and it gains energy when the reaction approaches PS. The decrease comes predominantly from the O4−H8 being broken; building up the connection O5−H5 is responsible for the nearly symmetric increase of O4 energy in the final stage. Both the bond energy and atom energy derivatives coherently describe these effects. For the O3 atom, the diagram shows quite different and nonsymmetric evolution: its energy derivative increases in the initial stage, as a consequence of the bond reorganization in the backbone, clearly reflected in Figure 3C. Detachment of H5 leads to strengthening the N−C and C−O bonds that will be washed out in the final stage by the attachment of H8 to O3, and thus, the oxygen atom will not lose energy upon final bond reorganization in the backbone, while the energy derivative of both N1 and C2 atoms will decrease considerably (Figure 3A).

The important feature on the relative energy derivatives of atoms and bonds alike for (**R3**) is strong confirmation of the effect found on the corresponding diagram for **R2**: here not only the bond energy diagrams (Figure 2C) but also diagrams for backbone atoms (N−C−O, Figure 2A) and fragility spectra (Figure 3B) clearly do not fall to zero at $\xi = 0$; the TS state is not a characteristic point for the structural changes in this reaction. The maxima and minima on the diagrams correspond only roughly to the reaction forces extremes (−0.41 and +0.36); meaningful variations on the energy derivatives are found even beyond the range of ξ (−1, + 1).

Diagonalization of the Connectivity Matrix. The connectivity matrix is singular (eq 4), but is nonetheless normal and its diagonalization can still be performed. The connectivity matrices have been diagonalized by the NumPy (v1.17.2) method[55,56] available online.[57] The matrix eigenvalues are presented in Table 2; due to the singular nature of the matrix (eq 4), one eigenvalue is zero for each structure (λ_o).

Table 2. Nonzero eigenvalues of the Connectivity Matrix (in au) for the Reactant State (RS), Transition State (TS) and Product State (PS) of the Internal Proton Transfer Reaction in Formamide (R2)

λ	RS	TS	PS
1	0.26	0.10	0.26
2	0.56	0.33	0.38
3	0.59	0.59	1.02
4	1.87	1.39	1.52
5	2.75	2.59	2.58

Results for the eigenvectors have been envisaged in three diagrams in Figure 4, describing the RS, TS, and PS for the internal proton transfer reaction in formamide molecule (**R2**) only. Calculated eigenvectors for nonzero eigenvalues have been standardized to one selected atom by the computational procedure, thus reminding, that the transformation of the coordinate system by the diagonalization procedure leads to nonidentical results for various states considered. As a consequence, the eigenvectors could not be compared as such between the reaction states RS, TS, and PS. However, the squares of the vectors (representing squares of their lengths), could be compared despite them belonging to a nonidentical coordinate system. All eigenvectors have been normalized to unity. This has provided a ground for the graphical representation of the eigenvectors in Figure 4. It contains atomic symbols (circles) of the diameter proportional to the modulus of the eigenvector component corresponding to this atom, its surface is proportional to the square of that eigenvector component. Because of eigenvectors normalization, the overall surface of circles for all atoms in each molecular diagram is identical in all diagrams and for all molecules. By this method, the qualitative and comparable pictorial representation of the involvement of atoms in eigenvectors on eigenvalues has been achieved.

Inspection of three diagrams in Figure 4 tends to confirm the leading role of the H4 atom movement in the reaction and also leads to a few additional interesting conclusions. The lowest energy eigenvectors in formamide RS (λ_1, λ_2) are characterized by not only the strongest involvement of H4 and O3 atoms, but also even more significant participation of the H5(N) and H6(C) atoms not active in the reaction. In the transition state (TS), the lowest energy eigenvector ($\lambda_1 = 0.10$) is dominated by the O3 and H4 atoms; however, the second one ($\lambda_2 = 0.33$) contains unusually high participation of the H6(C) atom as well. For the PS, which represents the acidic formamidine molecule, the lowest energy eigenvector ($\lambda_1 = 0.26$) contains considerable components from O and H4 atoms, and again comparable participation of H5(N) and H6(C) atoms. The eigenvectors corresponding to the highest energy eigenvalues in RS and PS molecules are dominated by the strongly bonded backbone atoms N−C−O, with reasonable participation of H4. In the TS structure, the oxygen atom, dominating at low energy level, plays no role in the highest energy eigenvector.

https://dx.doi.org/10.1021/acs.jpca.9b10145
J. Phys. Chem. A 2020, 124, 1076−1086

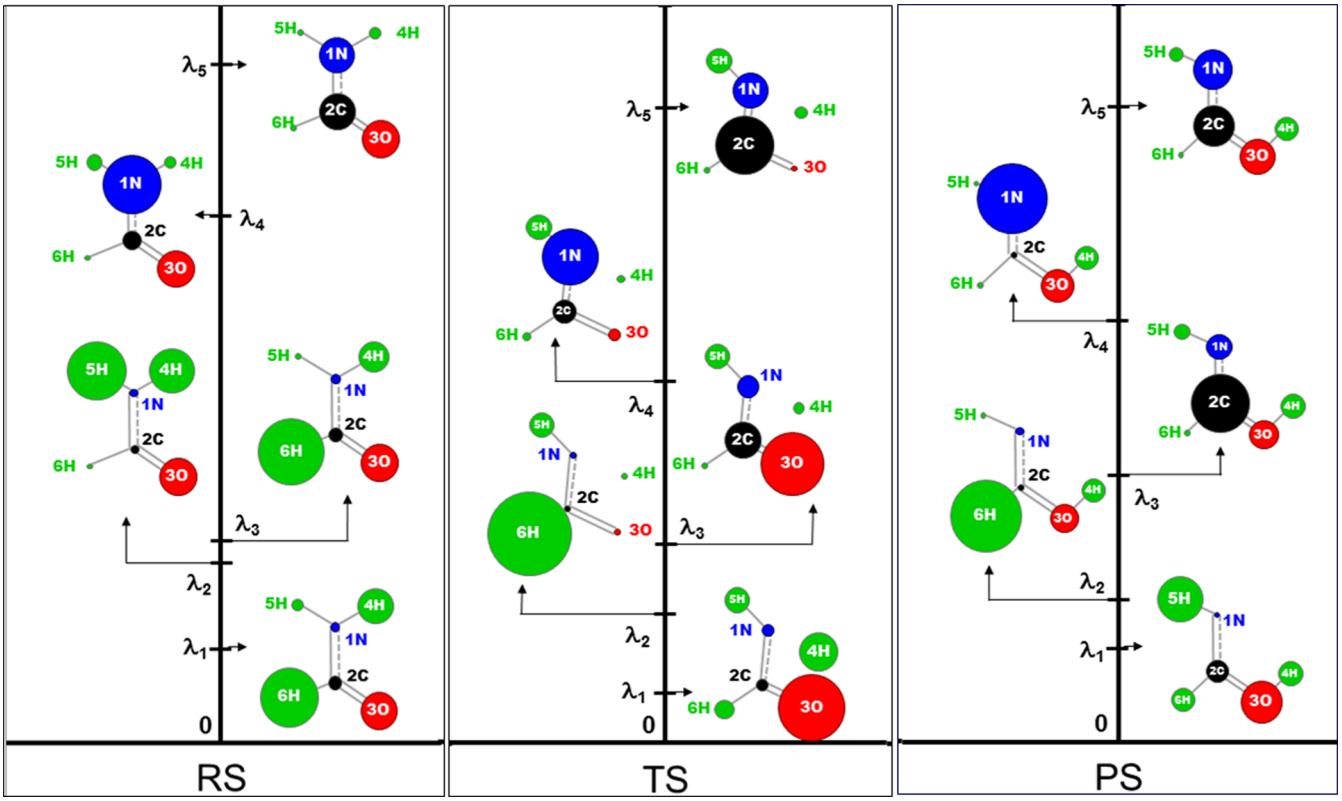

Figure 4. Representation eigenvectors corresponding to eigenvalues (λ, Table 2) of the connectivity matrix for the RS, TS, and PS states for the internal proton transfer reaction in formamide (**R2**).

5. CONCLUSION

The connectivity matrix, introduced and examined in former works,[39,43,44] appears to provide a wealth of chemical information on practical importance. The new general relation of the matrix diagonal elements to the electron density function (eq 8) convincingly demonstrates that their variations upon structural changes in a molecule studied along IRC (thus in a series of electronically stationary states) reflect evolution of the electron density function, responding to the variable geometry of nuclei. By our former finding, the matrix elements represent the sole electronic energy and they are free from components from nuclear repulsion forces.[39] This observation has opened a way to the reaction fragility (RF) spectra technique for monitoring the electron density changes in bonds and around atoms, that has since been proving its potential in studies of many reactions.[43,44,40] The method not only provides suggestive pictures for creating and/or breaking of real bonds in reacting systems, but also allows for monitoring any contact between atoms that affects the electron density in the space between them.

The energy analysis proposed in this present work provides yet a new tool: variation of energy derivative diagrams for an atom can be studied along a reaction, and variable energy of a bond can be observed as well. Although the Morse model was instrumental for the proof of the method, neither the Morse anharmonicity parameters, nor the atomization energies are needed for calculation of the ratio of the energy of an atom (V_A) or a bond (V_{AB}) to overall potential energy (V); the results rest entirely on the elements of the connectivity matrix, calculated at the desired level of quantum theory. Atomic/bond energy derivative diagrams appear to be even more powerful analytically than the fragility spectra: they manifest energy effects associated with the increase of density in the bond region and a change in bond energy resulting from the variable bond ionicity.

The results lead to several practical conclusions:

(i) Energy derivatives calculated for the internal rotation in formamide (**R1**) have shown how the density shift between atoms demonstrated in the fragility spectrum (C → O, C → N) results in selective bond strengthening (C−O) and weakening (C−N).

(ii) A competition between N and O atoms for the formation of a stronger bond with the central C atom upon the internal proton transfer in formamide (**R2**) observed in the energy derivative diagrams along the reaction path provides a formidable example of the analytic potential of the method.

(iii) The impact of variable ionicity of a bond has been observed in energy derivative diagrams for the double proton transfer reaction (e.g., in C−N, **R3**). Also, the diagrams for two various oxygen atoms in this system demonstrate high sensitivity of the method in exposing weak energetic effects.

(iv) The atom and bond energy derivative diagrams confirm a conclusion, earlier suggested by the RF spectra.[40,43,44] The transition state (TS) representing a maximum of global energy of a system is not the point of specific reorganization of bonds. This process occurs generally in the regions preceding and following the transition state; the turning points in energy attributed to bonds and atoms show no particular relation to the ones for global parameters of the system (e.g., energy and the reaction force). This observation supports the similar conclusion recently expressed by Nanayakkara and Kraka in their

https://dx.doi.org/10.1021/acs.jpca.9b10145
J. Phys. Chem. A 2020, 124, 1076−1086

work on joint application of the QTAIM and URVA methods to observation of a reaction dynamics.[20]

(v) Atomization energy, extensively explored in this present work, has been calculated as a difference: $D_{at}(\xi) = E(\xi) - \sum_A E_A$. Its derivative over the reaction progress (ξ) is thus equivalent to the reaction force, as introduced by Toro-Labbé et al.[22]

$$F_\xi = -\mathrm{d}E(\xi)/\mathrm{d}\xi = -\mathrm{d}D_{at}(\xi)/\mathrm{d}\xi \tag{19}$$

Separating the atomization energy into atomic contributions $D_{at}(\xi) = \sum_A D_{at,A}(\xi)$ (eq 16) opens a way to most natural separation of the reaction force itself to newly defined atomic contributions $F_\xi = \sum_A F_{\xi,A}$, a goal that has been attempted in the past[28,31] with a little success. The present result for an atomic share in the reaction force is straightforward:

$$F_{\xi,A} = -\mathrm{d}D_{at,A}(\xi)/\mathrm{d}\xi$$
$$\text{where } D_{at,A}(\xi) = [C_{AA}/Tr\underline{\underline{\mathbf{C}}}]D_{at}(\xi) \tag{20}$$

Considering the linear relation $\frac{1}{2}Tr\underline{\underline{\mathbf{C}}} = \alpha D_{at}$, the portion of the reaction force assigned to an atom is linked directly to the atomic RF, as defined in the original work[40] $a_\xi^A = \mathrm{d}C_{AA}/\mathrm{d}\xi$:

$$F_{\xi,A} = -\frac{1}{2\alpha}\mathrm{d}C_{AA}/\mathrm{d}\xi = -\frac{1}{2\alpha}a_\xi^A \tag{21}$$

The linear correlation parameter α warrants the coherence of units in the left-hand side and right-hand side of eq 21. This relation provides an interesting new interpretation for the atomic RF and the profiles thereof, by exposing their link to the novel concept of reaction forces attributed to atoms (eq 21).

(vi) Diagonalization of the connectivity matrix leads to a natural compartmentalization of the normal modes by combining them into eigenvalues of the connectivity matrix; the physical meaning of eigenvalues as the force constants remains unchanged as compared to Wilson transformation.[58] In the new eigenvectors the role of atoms has been exposed; the components of eigenvectors provide a measure of individual atoms involvement in deformation, associated with the given eigenvalue of the connectivity matrix (cumulative force constant[39]).

By introducing the method for monitoring the actual bond energies and their variations in reactions, this present work represents a step along the lines outlined by Politzer and Murray: "(...) *a chemical bond has no direct physical reality, but neither does energy. Yet the effects of both are physically evident and can be measured.*".[1] Calculation of the individual bond energy as a well-defined part of overall binding energy of a molecule provides additional support to the undoubtful reality of a chemical bond.

Observation of the energy of atoms-in-molecule demonstrated in this present work without atoms being defined *a priori* hints to an interesting problem of discovering the nature of these atoms; a question whether or not the electron density function could be divided into atomic contribution corresponding to atoms with energy fraction given by V_A/V remains a challenging task for the forthcoming studies. Atoms-in-molecule have never been "well cut", as noted by Mayer in his comprehensive article on bond orders and valence indices in quantum chemistry; this present work represents an effort toward "*interpretation and systematization of the results obtained in quantum chemical calculations*", that this author had considered necessary in order to "*extract from the wave function different pieces of information that may be assigned chemical significance*".

AUTHOR INFORMATION

Corresponding Author

Ludwik Komorowski − *Department of Physical and Quantum Chemistry, Wrocław University of Science and Technology, Wrocław 50-370, Poland;* orcid.org/0000-0003-2807-8101; Email: ludwik.komorowski@pwr.edu.pl

Authors

Piotr Ordon − *Department of Physics and Biophysics, Wrocław University of Environmental and Life Sciences, Wrocław 50-373, Poland;* orcid.org/0000-0002-7136-0367

Mateusz Jędrzejewski − *Department of Physical and Quantum Chemistry, Wrocław University of Science and Technology, Wrocław 50-370, Poland;* orcid.org/0000-0002-0467-5086

Jarosław Zaklika − *Department of Physical and Quantum Chemistry, Wrocław University of Science and Technology, Wrocław 50-370, Poland;* orcid.org/0000-0002-1322-4148

Complete contact information is available at: https://pubs.acs.org/10.1021/acs.jpca.9b10145

Notes

The authors declare no competing financial interest.

ACKNOWLEDGMENTS

The use of resources of Wrocław Center for Networking and Supercomputing is gratefully acknowledged (WCSS Grant No. 249 and GW 036).

REFERENCES

(1) Politzer, P.; Murray, J. S. A Look at Bonds and Bonding. *Struct. Chem.* **2019**, *30*, 1153−1157.

(2) Schrödinger, E. Quantisierung als Eigenwertproblem. *Ann. Phys.* **1926**, *384*, 361−376.

(3) Feynman, R. P. Forces in Molecules. *Phys. Rev.* **1939**, *56*, 340−343.

(4) Hohenberg, P.; Kohn, W. Inhomogeneous Electron Gas. *Phys. Rev.* **1964**, *136*, 864−871.

(5) Bader, R. F. W. Bond Paths Are Not Chemical Bonds. *J. Phys. Chem. A* **2009**, *113*, 10391−10396.

(6) Bader, R. F. W. The Density in Density Functional Theory. *J. Mol. Struct.: THEOCHEM* **2010**, *943*, 2−18.

(7) Bader, R. F. W. Pauli Repulsions Exist Only in the Eye of the Beholder. *Chem. - Eur. J.* **2006**, *12*, 2896−2901.

(8) Ivanic, J.; Atchity, G. J.; Ruedenberg, K. Intrinsic Local Constituents of Molecular Electronic Wave Functions. I. Exact Representation of the Density Matrix in Terms of Chemically Deformed and Oriented Atomic Minimal Basis Set Orbitals. *Theor. Chem. Acc.* **2008**, *120*, 281−294.

(9) Gilbert, A. T. B.; Gill, P. M. W.; Taylor, S. W. Extracting Atoms from Molecular Electron Densities via Integral Equations. *J. Chem. Phys.* **2004**, *120*, 7887−7893.

(10) Parr, R. G.; Ayers, P. W.; Nalewajski, R. F. What is an Atom in a Molecule? *J. Phys. Chem. A* **2005**, *109*, 3957−3959.

(11) Allen, T. L.; Shull, H. The Chemical Bond in Molecular Quantum Mechanics. *J. Chem. Phys.* **1961**, *35*, 1644−1651.

(12) Jacobsen, H. Chemical Bonding in View of Electron Charge Density and Kinetic Energy Density Descriptors. *J. Comput. Chem.* **2009**, *30*, 1093−1102.

(13) Foroutan-Nejad, C.; Shahbazian, S.; Marek, R. Toward a Consistent Interpretation of the QTAIM: Tortuous Link between Chemical Bonds, Interactions, and Bond/Line Paths. *Chem. - Eur. J.* **2014**, *20*, 10140−10152.
(14) Gillespie, R. J.; Robinson, E. A. Gilbert N. Lewis and the Chemical Bond: The Electron Pair and the Octet Rule from 1916 to the Present Day. *J. Comput. Chem.* **2007**, *28*, 87−97.
(15) Fukui, K. The Path of Chemical Reactions - the IRC Approach. *Acc. Chem. Res.* **1981**, *14*, 363−368.
(16) Miller, W. H.; Handy, N. C.; Adams, J. E. Reaction Path Hamiltonian for Polyatomic molecules. *J. Chem. Phys.* **1980**, *72*, 99−112.
(17) Piela, L. *Ideas of Quantum Chemistry*; Elsevier: Amsterdam N. L., 2007.
(18) López, J. G.; Vayner, G.; Lourderaj, U.; Addepalli, S. V.; Kato, S.; deJong, W. A.; Windus, T. L.; Hase, W. L. A Direct Dynamics Trajectory Study of F^- + CH3OOH Reactive Collisions Reveals a Major Non-IRC Reaction Path. *J. Am. Chem. Soc.* **2007**, *129*, 9976−9985.
(19) Klippenstein, S. J.; Pande, V. S.; Truhlar, D. G. Chemical Kinetics and Mechanisms of Complex System: A Perspective on Recent Theoretical Advances. *J. Am. Chem. Soc.* **2014**, *136*, 528−546.
(20) Nanayakkara, S.; Kraka, E. A New Way of Studying Chemical Reactions: a Hand-in-hand URVA and QTAIM Approach. *Phys. Chem. Chem. Phys.* **2019**, *21*, 15007−15018.
(21) Toro-Labbé, A. Characterization of Chemical Reactions from the Profiles of Energy, Chemical Potential, and Hardness. *J. Phys. Chem. A* **1999**, *103*, 4398−4403.
(22) Toro-Labbé, A.; Gutiérrez-Oliva, S.; Murray, J. S.; Politzer, P. A new Perspective on Chemical and Physical Processes: The Reaction Force. *Mol. Phys.* **2007**, *105*, 2619−25.
(23) Toro-Labbé, A.; Gutiérrez-Oliva, S.; Politzer, P.; Murray, J. S. Reaction Force: A Rigorously Defined Approach to Analyzing Chemical and Physical Processes. In *Chemical Reactivity Theory. A density functional Viewpoint*; Chattaraj, P. K., Ed.; CRC Press, Taylor & Francis Group: Boca Raton, FL, 2009.
(24) Politzer, P.; Toro-Labbé, A.; Gutiérrez-Oliva, S.; Murray, J. S. Perspectives on the Reaction Force. In *Advanced Quantum Chemistry*; Sabin, J. R., Brändas, E. J., Eds.; Elsevier: Amsterdam, N.L., 2012; Vol. *64*.
(25) Konkoli, Z.; Kraka, E.; Cremer, D. Unified Reaction Valley Approach Mechanism of the Reaction CH_3+H_2 → CH_4+H. *J. Phys. Chem. A* **1997**, *101*, 1742−1757.
(26) Konkoli, Z.; Cremer, D. A New Way of Analyzing Vibrational Spectra. I. Derivation of Adiabatic Internal Modes. *Int. J. Quantum Chem.* **1998**, *67*, 1−9.
(27) Cremer, D.; Wu, A.; Kraka, E. The Mechanism of the Reaction FH + H C CH → H C− CFH. Investigation of Hidden Intermediates with the Unified Reaction Valley Approach. *Phys. Chem. Chem. Phys.* **2001**, *3*, 674−687.
(28) Inostroza-Rivera, R.; Yahia-Ouhmed, M.; Tognetti, V.; Joubert, L.; Herrera, B.; Toro- Labbé, A. Atomic Decomposition of Conceptual DFT Descriptors: Application to Proton Transfer Reactions. *Phys. Chem. Chem. Phys.* **2015**, *17*, 17797−807.
(29) Vöhringer-Martinez, E.; Toro- Labbé, A. Understanding the Physics and Chemistry of Reaction Mechanisms from Atomic Contributions: A Reaction Force Perspective. *J. Phys. Chem. A* **2012**, *116*, 7419−7423.
(30) Pendas, A. M.; Blanco, M. A.; Francisco, E. Two Electron Integrations in the Quantum Theory of Atoms in Molecules. *J. Chem. Phys.* **2004**, *120*, 4581−92.
(31) Jędrzejewski, M.; Ordon, P.; Komorowski, L. Atomic Resolution for the Energy Derivatives on the Reaction Path. *J. Phys. Chem. A* **2016**, *120*, 3780−3787.
(32) Kraka, E.; Cremer, D. Computational Analysis of the Mechanism of Chemical Reactions in Terms of Reaction Phases: Hidden Intermediates and Hidden Transition States. *Acc. Chem. Res.* **2010**, *43*, 591−601.
(33) Zou, W.; Sexton, T.; Kraka, E.; Freindorf, M.; Cremer, D. A New Method for Describing the Mechanism of a Chemical Reaction Based on the Unified Reaction Valley Approach. *J. Chem. Theory Comput.* **2016**, *12*, 650−663.
(34) Cremer, D.; Wu, A.; Kraka, E. The Mechanism of the Reaction FH + H C CH → H C− CFH. Investigation of Hidden Intermediates with the Unified Reaction Valley Approach. *Phys. Chem. Chem. Phys.* **2001**, *3*, 674−687.
(35) Ordon, P. *Effect of molecular deformations on the chemical DFT indices*. Ph.D. Thesis, Wrocław University of Technology, 2003.
(36) Ordon, P.; Tachibana, A. Use of Nuclear Stiffness in Search for a Maximum Hardness Principle and for the Softest States along the Chemical Reaction Path: A New Formula for the Energy Third Derivative γ. *J. Chem. Phys.* **2007**, *126*, 234115.
(37) Ordon, P.; Tachibana, A. New Reactivity Indices within Regional Density Functional Theory. *J. Mol. Model.* **2005**, *11*, 312−316.
(38) Ordon, P.; Tachibana, A. Investigation of the Role of the C-PCM Solvent Effect in Reactivity Indices. *Proc. - Indian Acad. Sci., Chem. Sci.* **2005**, *117*, 583−589.
(39) Ordon, P.; Komorowski, L.; Jędrzejewski, M. Conceptual DFT Analysis of the Fragility Spectra of Atoms along the Minimum Energy Reaction Coordinate. *J. Chem. Phys.* **2017**, *147*, 134109.
(40) Komorowski, L.; Ordon, P.; Jędrzejewski, M. The Reaction Fragility Spectrum. *Phys. Chem. Chem. Phys.* **2016**, *18*, 32658−32663.
(41) Mayer, I. Bond Order and Valence Indices. *J. Comput. Chem.* **2007**, *28*, 204−221.
(42) Ordon, P.; Zaklika, J.; Jędrzejewski, M.; Komorowski, L. Bond Softenning Indices Studied by the Fragility Spectra for Proton Migration in Formamide and related Structures. *J. Phys. Chem. A* **2020**, *124*, 328−338.
(43) Zaklika, J.; Komorowski, L.; Ordon, P. Evolution of the Atomic Valence Observed by the Reaction Fragility Spectra on the Reaction Path. *J. Mol. Model.* **2019**, *25*, 134.
(44) Zaklika, J.; Komorowski, L.; Ordon, P. The Bond Fragility Spectra for the Double Proton Transfer Reaction, in the Formic Acid Type Dimers. *J. Phys. Chem. A* **2019**, *123*, 4274−4283.
(45) Liu, S.; Parr, R. G.; Nagy, A. Cusp Relations for Local Strongly Decaying Properties in Electronic Systems. *Phys. Rev. A: At., Mol., Opt. Phys.* **1995**, *52*, 2645−2651.
(46) Kato, T. On the Eigenfunctions of Many-particle Systems in Quantum Mechanics. *Commun. Pure Appl. Math.* **1957**, *10*, 151−177.
(47) Chattaraj, P. K.; Cedillo, A.; Parr, R. G. Fukui Function for a Gradient Expansion Formula, and Estimate of Hardness and Covalent Radius for an Atom. *J. Chem. Phys.* **1995**, *103*, 10621−10626.
(48) Atkins, P. W. *Physical Chemistry*, 6th ed.; Oxford University Press, 1998.
(49) Frisch, M. J.; Trucks, G. W.; Schlegel, H. B.; Scuseria, G. E.; Robb, M. A.; Cheeseman, J. R.; Scalmani, G.; Barone, V.; Mennucci, B.; Petersson, G. A.; Nakatsuji, H.; Caricato, M.; Li, X.; Hratchian, H. P.; Izmaylov, A. F.; Bloino, J.; Zheng, G.; Sonnenberg, J. L.; Hada, M.; Ehara, M.; Toyota, K.; Fukuda, R.; Hasegawa, J.; Ishida, M.; Nakajima, T.; Honda, Y.; Kitao, O.; Nakai, H.; Vreven, T.; Montgomery, J. A., Jr.; Peralta, J. E.; Ogliaro, F.; Bearpark, M.; Heyd, J. J.; Brothers, E.; Kudin, K. N.; Staroverov, V. N.; Kobayashi, R.; Normand, J.; Raghavachari, K.; Rendell, A.; Burant, J. C.; Iyengar, S. S.; Tomasi, J.; Cossi, M.; Rega, N.; Millam, J. M.; Klene, M.; Knox, J. E.; Cross, J. B.; Bakken, V.; Adamo, C.; Jaramillo, J.; Gomperts, R.; Stratmann, R. E.; Yazyev, O.; Austin, A. J.; Cammi, R.; Pomelli, C.; Ochterski, J. W.; Martin, R. L.; Morokuma, K.; Zakrzewski, V. G.; Voth, G. A.; Salvador, P.; Dannenberg, J. J.; Dapprich, S.; Daniels, A. D.; Farkas, O.; Foresman, J. B.; Ortiz, J. V.; Cioslowski, J.; Fox, D. J. *Gaussian 09*, revision A.02;Gaussian Inc.: Wallingford, CT, 2009.
(50) Fu, A.-p.; Li, H.-l.; Du, D.-m.; Zhou, Z.-y. Theoretical Study on the Reaction Mechanism of Proton Transfer in Formamide. *Chem. Phys. Lett.* **2003**, *382*, 332−337.
(51) Wang, X.-C.; Nichols, J.; Feyereisen, M.; Gutowski, M.; Boatz, J.; Haymet, A. D. J.; Simons, J. Ab Initio Quantum Chemistry Study of Formamide-Formamidic Acid Tautomerization. *J. Phys. Chem.* **1991**, *95*, 10419−10424.

https://dx.doi.org/10.1021/acs.jpca.9b10145
J. Phys. Chem. A 2020, 124, 1076−1086

(52) Zaspel, P.; Huang, B.; Harbrecht, H.; von Lilienfeld, O. A. Boosting Quantum Machine Learning Models with a Multilevel Combination Technique: Pople Diagrams Revisited. *J. Chem. Theory Comput.* **2019**, *15*, 1546−1559.
(53) Csonka, G. I.; Ruzsinszky, A.; Tao, J.; Perdew, J. P. Energies of Organic Molecules and Atoms in Density Functional Theory. *Int. J. Quantum Chem.* **2005**, *101*, 506−511.
(54) Komorowski, L.; Ordon, P. Vibrational Softening of Diatomic Molecules. *Theor. Chem. Acc.* **2001**, *105*, 338−344.
(55) Oliphant, T. E. *A guide to NumPy*; Trelgol Publishing:USA, 2006.
(56) van der Walt, S.; Colbert, C. S.; Varoquaux, G. The NumPy Array: A Structure for Efficient Numerical Computation. *Comput. Sci. Eng.* **2011**, *13*, 22−30.
(57) numpy. The fundamental package for scientific computing with Python. https://github.com/numpy/numpy/tree/v1.17.2 (accessed 2019.10.28).
(58) Wilson, E. B., Jr.; Decius, J. C.; Cross, P. C. *Molecular Vibrations*; Dover Publications: New York, USA, 1980.

https://dx.doi.org/10.1021/acs.jpca.9b10145
J. Phys. Chem. A 2020, 124, 1076−1086